Biophysical Journal Volume 96 June 2009 4725–4732

Cytoskeletal Polymer Networks: Viscoelastic Properties are Determined by the Microscopic Interaction Potential of Cross-links

O. Lieleg,[†‡] K. M. Schmoller,[†] M. M. A. E. Claessens,[†§] and A. R. Bausch[†*]

[†]Lehrstuhl für Zellbiophysik E27, Technische Universitt München, Garching, Germany; [‡]Faculty of Arts and Sciences, Center for Systems Biology, Harvard University, Cambridge, Massachusetts; and [§]Biophysical Engineering Group, MESA+ Institute for Nanotechnology, Faculty of Science and Technology, University of Twente, Enschede, The Netherlands

ABSTRACT Although the structure of cross-linking molecules mainly determines the structural organization of actin filaments and with that the static elastic properties of the cytoskeleton, it is largely unknown how the biochemical characteristics of transiently cross-linking proteins (actin-binding proteins (ABPs)) affect the viscoelasticity of actin networks. In this study, we show that the macroscopic network response of reconstituted actin networks can be traced back to the microscopic interaction potential of an individual actin/ABP bond. The viscoelastic response of cross-linked actin networks is set by the cross-linker off-rate, the binding energy, and the characteristic bond length of individual actin/ABP interactions.

INTRODUCTION

Cells employ cross-linked and bundled actin networks to form an elastic cytoskeleton that can withstand mechanical load. Transient cross-links guarantee structural and mechanical adaptability at long timescales while ensuring an elastic network response at timescales that are short compared to the cross-linker off-rate (1). Nature offers a huge variety of actin-binding proteins (ABPs) to tailor the microstructure and the mechanical properties of the cytoskeleton. To achieve high versatility, cells make use of the inherent biochemical differences of diverse ABPs. These differences manifest themselves in distinct interaction potentials, which above all can be manipulated by forces acting on the actin/ABP bond—a strategy that cells can pursue by creating internal stresses (2). To shed light on the link between the biochemical diversity of cross-linking proteins and the mechanical response of the cytoskeleton, one needs to address the underlying physical principles. For this purpose, in vitro model systems have been proven essential (3). Depending on the microstructure of such reconstituted networks, a macroscopic deformation can be transmitted to the microscopic level of single filaments and individual cross-linking molecules in an affine or nonaffine manner (4–8). In either case, large forces can evoke rupturing of the actin/ABP bond (6,9), which further complicates the complex nonlinear behavior of actin networks (10–12). In a previous study, we have shown that in the absence of external or internal forces, thermal energy is sufficient to entail cross-linker unbinding events, which determine the dynamic network response at low frequencies (13). While it has been shown that the static elastic response of cross-linked actin networks depends crucially on the structure and size of the cross-linking molecules (14), the dynamic viscoelastic response should sensitively depend on the microscopic interaction potential of actin/ABP bonds. The dynamic interplay between actin filaments and ABPs is set by biochemical parameters such as the binding energy E_B, the cross-linker on- and off-rate k_{on} and k_{off}, and the position of the transition state Δx, which represents the characteristic bond length (Fig. 1). Typically, these parameters are determined by a combination of biochemical and single molecule studies (15,16). For further progress in a microscopic understanding of cellular mechanics, it needs to be shown whether these biochemical properties of the cross-linking molecules are closely linked to their mechanical function.

In this study, we demonstrate that the macromechanical response of transiently cross-linked actin networks sensitively depends on the interaction potential of single actin/ABP bonds. While the static network elasticity can be rationalized by the network microstructure, we show that the biochemical properties of single cross-links dictate the frequency response of transiently cross-linked actin networks. For a detailed analysis of this frequency response, we choose rigor-heavy meromyosin (HMM) as an actin cross-linking molecule. Rigor-HMM creates isotropically cross-linked actin networks, which are ideally suited to quantify the impact of microscopic cross-linker unbinding events on the macroscopic network response. Here, the dependence of the viscoelastic network response on the cross-linker concentration, temperature, and external force is traced back to key parameters of the actin/HMM interaction potential, which characterizes the unbinding process of the actin/HMM bond. The off-rate, the binding energy, and the position of the transition state are quantitatively determined from the viscoelastic frequency spectrum of the network by utilizing a microscopic model, which is predicated on single unbinding events.

MATERIALS AND METHODS

Protein preparation

G-actin is obtained from rabbit skeletal muscle and stored in lyophilized form at −21°C (17). For measurements, the lyophilized actin is dissolved

Submitted November 14, 2008, and accepted for publication March 11, 2009.

*Correspondence: abausch@ph.tum.de

Editor: Marileen Dogterom.

0006-3495/09/06/4725/8 $2.00

doi: 10.1016/j.bpj.2009.03.038

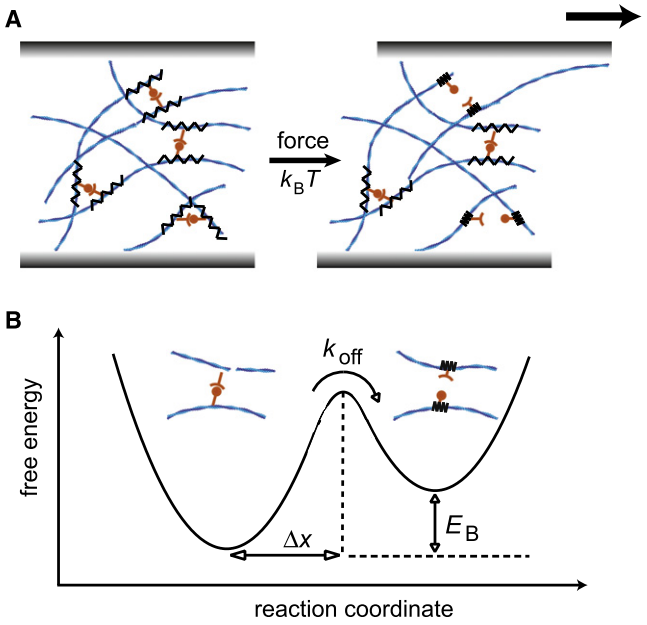

FIGURE 1 (*A*) In cross-linked actin networks, a transient bond can unbind because of thermal activation, k_BT, or upon force application. (*B*) The transient actin/ABP cross-link can be characterized by an interaction potential. The key parameters are the cross-linker off-rate, k_{off}, the binding energy, E_B, and the position of the transition state, Δx.

in deionized water and dialyzed against G-Buffer (2 mM Tris, 0.2 mM ATP, 0.2 mM $CaCl_2$, 0.2 mM DTT, and 0.005% NaN_3, pH 8) at 4°C. The G-actin solutions are kept at 4°C and used within seven days of preparation. The average length of the actin filaments is controlled to 21 μm using gelsolin obtained from bovine plasma serum, following Kurokawa et al. (18). HMM is prepared from myosin II by chymotrypsin digestion and tested using motility assays, as in Uhde et al. (19).

Rheology

The viscoelastic response of actin/HMM-networks is determined by measuring the frequency-dependent viscoelastic moduli $G'(f)$ and $G''(f)$ with a stress-controlled rheometer (Physica MCR 301; Anton Paar, Graz, Austria) over a frequency range of three decades. Approximately 500 μL sample volume is loaded within 1 min into the rheometer using a 50-mm plate-plate geometry with 160-μm plate separation. To ensure linear response, small torques ($\approx$0.5 μN m) are applied. The transition to rigor HMM upon ATP depletion is followed by recording the elastic response G'(0.5 Hz) of the actin/HMM network in time. In the experiments, the molar ratio R between HMM and actin, $R = c_{HMM}/c_a$, is varied; actin polymerization is carried out in situ, as described before in Luan et al. (20). To determine the force dependence of the viscoelastic response, increasing amounts of constant prestress σ_0 are applied. Only densely cross-linked networks are investigated under prestress to avoid plastic deformation during the measurement. Full relaxation of the network is ensured in between two prestress measurements. The frequency dependence of $G'(f)$ and $G''(f)$ is determined with an oscillating measuring stress $\sigma_m(t) = \sigma_m^0 \times \sin(2\pi f \cdot t)$, whereas $\sigma_m^0 = 0.2 \times \sigma_0$.

Data analysis

Microscopic parameters such as the cross-linker off-rate are obtained from the experimental frequency spectra by globally fitting the following equations to each set of measurements:

$$G'(f) = G_0 - a \times \frac{Nk_{off}}{\frac{k_{off}^2}{4\pi^2} + f^2} + b \times \left(\frac{f}{f_0}\right)^{3/4}, \quad (1)$$

$$G''(f) = c \times \frac{Nf}{\frac{k_{off}^2}{4\pi^2} + f^2} + d \times \left(\frac{f}{f_0}\right)^{3/4}. \quad (2)$$

In brief, N denotes the number of cross-links formed and k_{off} denotes the off-rate of the cross-link. The first term containing the prefactors a and c describes the amount of energy that is dissipated because of cross-link unbinding, whereas the second term containing the prefactors b and d represents the fluctuation of single filaments in semiflexible polymer networks. The timescale of this second relaxation mode is set by the factor f_0, which is a function of the solvent viscosity η and the filament density but is fixed to 1 Hz for most of the experiments. A detailed derivation of these equations including a full discussion of all involved parameters is given in Lieleg et al. (13). As also discussed there, this model can quantitatively reproduce the frequency response of a cross-linked network for frequencies $f \geq f_{max}$, where $f_{max} = k_{off}/2\pi$ denotes the frequency of maximal low frequency dissipation. At lower frequencies, a third microscopic mechanism has to be considered that is not captured by this model. The detailed values of all fitting parameters are given in the Appendix. It is important to note that $\frac{a}{c}$ = const. and $\frac{b}{d}$ = const. for all experiments, which significantly reduces the number of free fitting parameters.

RESULTS AND DISCUSSION

Actin networks formed by rigor-HMM are homogeneous and isotropically cross-linked. Therefore, the network elasticity depends solely on one length scale, which is the cross-linker distance l_c (6,20). However, it is important to note that the formed cross-links are not covalent: they can unbind and rebind. The transient nature of actin/HMM cross-links becomes evident in a step-stress experiment. Such an experiment is conducted for a strongly cross-linked actin/HMM network ($R = 0.1$) as depicted in Fig. 2 *A*. At intermediate timescales ($\approx$40–60 s), the network exhibits significant creep, which does not entail plastic deformation of the network. Multiple un- and rebinding events of cross-linking molecules follow the direction of force application, during which the overall network microstructure is preserved, giving rise to a well-reproducible network response. Yet, the occurrence of significant creep behavior in a densely cross-linked network clearly demonstrates the transient character of the cross-links.

This transient nature of the formed cross-links is underlined by a second observation: at intermediate frequencies, i.e. between 0.1 Hz and 1 Hz, transiently cross-linked actin/HMM networks exhibit a minimum in the loss modulus $G''(f)$ (6,9), which characterizes the viscous dissipation. As shown before, this minimum results from the competition of thermally activated cross-link unbinding events at low frequencies and the fluctuation of single filaments at high frequencies. It can be suppressed if the cross-link is stabilized by a covalent linkage (13). For isotropically cross-linked networks as formed by rigor-HMM, the minimum in the

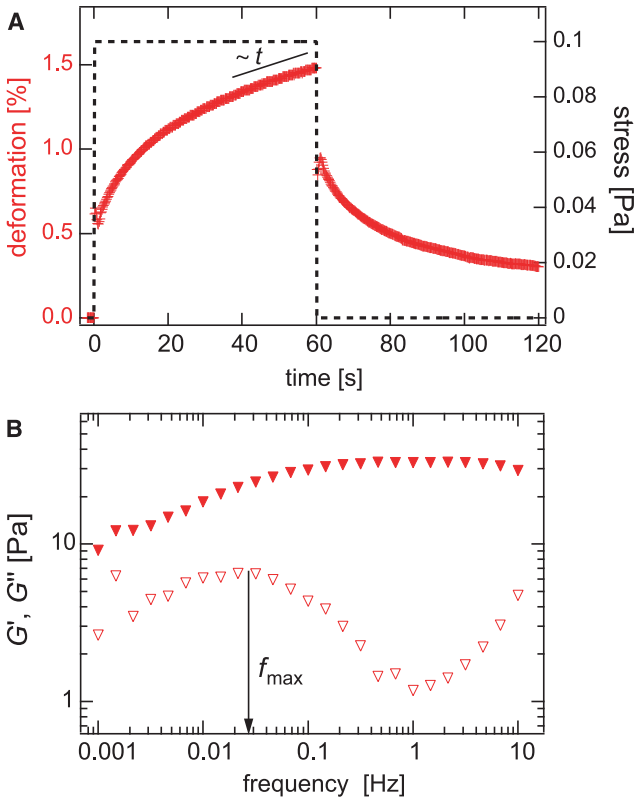

FIGURE 2 The transient nature of actin/HMM cross-links dictates the viscoelastic response of the macroscopic network. (*A*) A stress pulse of 0.1 Pa height and 60 s duration is applied to a transiently cross-linked actin/HMM network ($R = 0.1$, $c_a = 9.5$ μM) and the resulting deformation is recorded. This step-stress experiment reveals significant creep behavior at timescales of ≈40–60 s. (*B*) Extended frequency spectrum of a transiently cross-linked actin/HMM network ($R = 0.1$, $c_a = 9.5$ μM). A clear maximum in the viscous dissipation is located at $f_{max} \approx 0.03$ Hz.

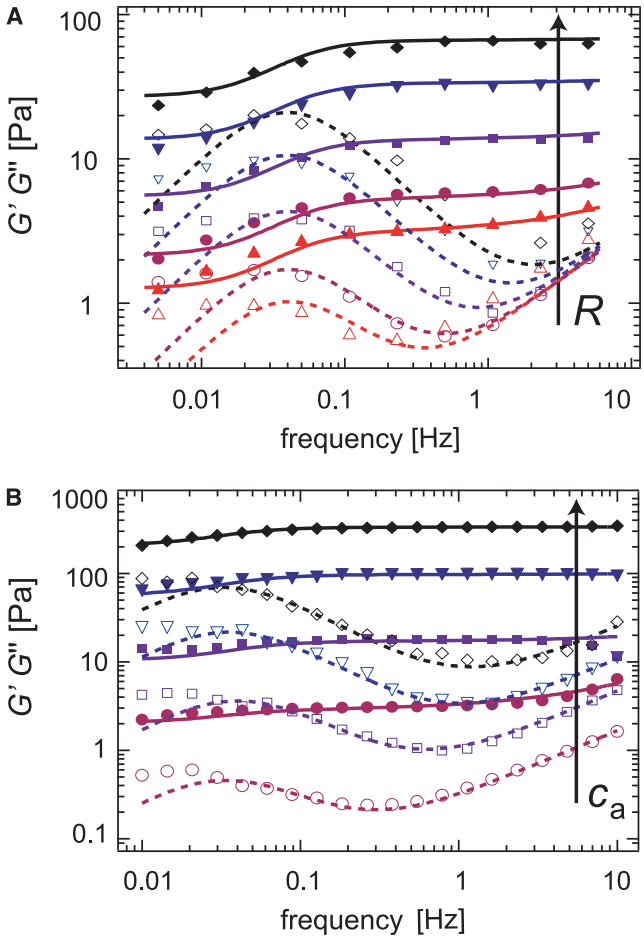

FIGURE 3 Either a cross-linker concentration series (*A*, fixed $c_a = 19$ μM, variable $R = 0.0076$, 0.0152, 0.0385, 0.0714, and 0.143) or an actin concentration series (*B*, fixed $R = 0.1$, variable $c_a = 4.75$ μM, 9.5 μM, 19 μM, and 28.5 μM) can be employed to extract the cross-linker off-rate from the viscoelastic spectrum of transiently cross-linked actin/HMM networks. Solid symbols denote $G'(f)$, open symbols denote $G''(f)$. The solid and dashed lines represent a global best fit using Eqs. 1 and 2 as described in the Appendix.

viscous dissipation is well pronounced—its exact position depends on both the actin concentration and the cross-linker density R, as depicted in Fig. 3. At low frequencies, a maximum in the viscous dissipation is detectable, whose position f_{max} is independent from R. It is important to note that, in this low frequency regime, the network response is still dominated by elasticity, which is consistent with the significant recovery of the network upon stress release (Fig. 2 *A*). The frequency spectra of isotropically cross-linked actin/HMM networks can be quantitatively reproduced by a semi-phenomenological model, which was introduced in Lieleg et al. (13). In this article we demonstrate, step-by-step, how this model can be employed to determine the microscopic interaction potential of actin/HMM cross-links from the macroscopic network response of cross-linked actin/HMM networks. To validate the obtained results, a comparison with independently obtained parameter values is crucial. The biochemical interaction of actin and rigor HMM has been characterized in great detail (21). This makes actin/HMM networks ideal for a quantitative analysis of the viscoelastic network response.

In a cross-linker concentration series as depicted in Fig. 3 *A*, the cross-linker off-rate is constant, which makes this set of measurements perfectly suitable to determine k_{off}. The total number of cross-links N is set by experimental conditions. As discussed before (6,13), the scaling relation $G_0 \sim \kappa_0^2/k_B T \xi^2 l_c^3 \sim N$ describes the static network elasticity G_0 on the basis of microscopic parameters such as the actin filament bending stiffness κ_0, the network mesh size ξ, and the average cross-linker distance l_c, utilizing an affine stretching model (22). In essence, this relation correlates the number of cross-links N with the macroscopic network elasticity. With the experimental constraint $G_0 \sim R^{1.2}$ (6,20), the best reproduction of the data set is obtained for $k_{off} \approx (0.30 \pm 0.05)$ s^{-1}. A similar result is obtained if the actin concentration is varied at a fixed cross-linker concentration (e.g., $R = 0.1$), as depicted in Fig. 3 *B*. Here, $k_{off} \approx (0.23 \pm 0.05)$ s^{-1} is obtained, which agrees well

with both the result obtained from the R-series and values determined by biochemical means (21). Note that in the actin concentration series, the impact of single filament fluctuations becomes more pronounced with increasing actin concentrations. Consistently, the single filament fluctuation parameter d depends roughly linear on the actin concentration—representing the increasing density of actin filaments. At higher filament densities the entanglement length decreases, which facilitates the formation of cross-links at a given cross-linker concentration. Thus, in the actin concentration series, the effective cross-link density is increased as well. This makes this experiment qualitatively very similar to the R-series discussed before. In both cases, the variation of the cross-link density allows for the extraction of the cross-linker off-rate of individual actin/HMM bonds. This finding confirms that the timescale at which the energy dissipation in the cross-linked network is minimal is set not only by the static density of the cross-links but also by the dynamic off-rate of the actin/ABP bond.

In addition, since cross-link unbinding determines the frequency response of transiently cross-linked networks, the characteristic binding energy of the cross-link should be obtainable from temperature dependent frequency sweeps. The results depicted in Fig. 3 demonstrate that thermal energy is sufficient to drive the actin/HMM bond across the potential barrier. The binding energy E_B is dissipated every time an unbinding event occurs between the cross-linking molecule and the actin filament. E_B characterizes the cross-link and sets the total ratio of bound/unbound molecules. This gives rise to an inherent temperature dependence of the binding constant $K(T) \sim \exp(-E_B/k_BT)$. Thus, investigating the frequency spectrum of a cross-linked actin network at different temperatures should be an appropriate approach to determine the binding energy of a single cross-link.

We conduct a series of linear response measurements in a temperature range of 10–30°C, as depicted in Fig. 4 *A*. Starting at 21°C, where the network has been polymerized, we vary the sample temperature using a protocol of oscillating temperature steps ($T = 21°C \rightarrow 15°C \rightarrow 25°C \rightarrow 10°C \rightarrow 30°C$), providing adequate time for thermal equilibration (Fig. 4 *C*). This protocol guarantees that a putative change in the observed network response is purely due to thermal effects and not superimposed by time-dependent changes like sample aging. As depicted in Fig. 4 *A*, a continuous decrease in both viscoelastic moduli is observed with increasing temperature T. Within the fitting accuracy, a reproduction of the data set by the model described in Lieleg et al. (13) results in an approximately constant off-rate, $k_{off} \approx 0.3\ s^{-1}$, although a small variation of k_{off} with temperature within a factor of 2 would still be consistent with the data. This is in contrast to actin/α-actinin-4 networks (23), where a strong dependence of this off-rate (called ''network relaxation frequency'' in (23)) on temperature is observed. Furthermore, a decrease of the static elasticity G_0 with increasing T (Fig. 4 *B*) and a shift of the timescale of the single filament relaxation regime, $t_0 = 1/f_0$ (13), is observed. This time can be normalized by the solvent viscosity η yielding $\frac{t_0}{\eta}$. This parameter is almost independent of T (Fig. 4 *B*), indicating that the observed shift of this timescale with respect to T is simply given by the temperature dependence of the solvent viscosity.

As the static plateau modulus G_0 of isotropically cross-linked actin networks depends solely on the total number of intact cross-links, the experimental scaling relation $G_0 \sim R^{1.2}$ (6,20) can be rewritten using the number of effectively bound cross-linker molecules R_{eff}. With the binding constant of rigor-HMM to actin $K = 1.2 \times 10^6\ M^{-1}$ (21) we obtain $G_0 = 157\ Pa \times R_{eff}^{1.1}$ for $c_a = 9.5\ \mu M$ (6). Using the law of mass action, R_{eff} can be calculated as a function of R and K:

$$R_{eff} = \frac{1}{2}\left[\left(1 + R + \frac{1}{c_a K(T)}\right) - \sqrt{\left(1 + R + \frac{1}{c_a K(T)}\right)^2 - 4R}\right].$$

With the temperature dependence of the binding constant K, the binding energy of the actin/HMM bond can be numerically extracted from the $G_0(R_{eff}(T))$ data depicted in Fig. 4 *B* to be $E_B \approx (-40 \pm 4)\ kJ \times mol^{-1}$—in excellent agreement with the literature value of $(-39 \pm 1)\ kJ \times mol^{-1}$ (24). A similar temperature dependence was reported for actin

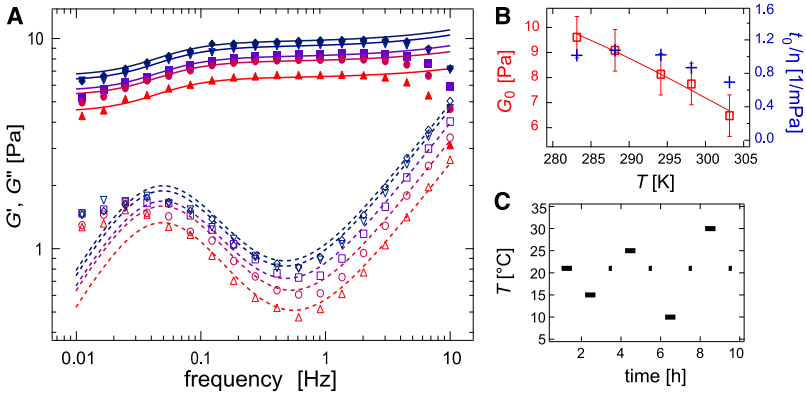

FIGURE 4 (*A*) Frequency response of actin/HMM networks ($c_a = 9.5\ \mu M$, $R = 0.1$) at distinct temperatures (10°C (◇) up to 30°C (△)). Solid symbols denote $G'(f)$, open symbols denote $G''(f)$. The solid and dashed lines represent the model used to evaluate the macromechanical response, as described in Lieleg et al. (13). (*B*) Plateau modulus G_0 (□) and the normalized time t_0/η (+) as a function of temperature. The character η denotes the viscosity of water. (*C*) Temperature-oscillation protocol as described in the article. Frequency sweeps (*bars*) are taken at 21°C, 15°C, 25°C, 10°C, and 30°C. Before the next temperature jump is initiated, the network is brought back to its initial temperature of 21°C to assure reversibility (*dots*).

networks cross-linked by α-actinin (25). There, the complicated and heterogeneous microstructure of α-actinin networks defied a quantitative comparison of the macroscopic network elasticity with the cross-linker affinity. However, our results on actin/HMM networks clearly demonstrate that the binding energy of a single cross-link determines the temperature dependence of the network response of transiently cross-linked actin networks.

Although cells can react only passively to changes in the temperature of their environment, adjusting the local density or composition of cross-linking molecules gives them the possibility to actively tune their mechanical properties. Another strategy to actively control cytoskeletal mechanics is given by creating internal forces. It was shown that living cells exploit molecular motors to create and maintain a certain level of internal stress to increase the elastic response of the cytoskeleton (2). However, it remains to be analyzed how external or internal forces acting on cytoskeletal networks affect the binding kinetics of cross-linking molecules and therefore the dynamic viscoelastic network response.

A microscopic parameter dictating the sensitivity of a transient actin/ABP bond toward forces is the characteristic bond length, Δx. This parameter marks the position of the transition state of the binding/unbinding process. Having demonstrated that the viscoelastic response of a transiently cross-linked actin/HMM network is set by the off-rate and the binding energy of the actin/HMM bond, it is now addressed whether the bond length Δx influences the network mechanics. If this is the case, the bond length should be obtainable from the macroscopic network response by employing the force dependence of the binding kinetics of the cross-linker.

For cross-linked bundle networks as they are formed by the ABP fascin, it has been shown that the rupture force of an actin/fascin bond depends on the loading rate in a logarithmic manner (9), as expected from single molecule experiments (26). There, a variation of the force loading rate allows for shifting the rupture force distribution and thus determining Δx. A similar principle should also be applicable here; however, instead of studying the loading rate dependence of the rupture force, the application of a constant prestress (11) should already be sufficient to characterize the cross-link unbinding process in the presence of external force, provided that plastic deformations are avoided. Therefore, the frequency dependence of the viscoelastic network response of densely cross-linked actin/HMM networks ($R = 0.1$ and $R = 0.2$) in the presence of varying external prestress σ_0 is analyzed (Fig. 5, *A* and *B*).

As depicted in Fig. 6 *A*, the static network elasticity increases linearly with the prestress, $G_0 \sim \sigma_0$. Furthermore, the global fit of the prestress series requires an increase of both stress relaxation parameters $a(\sigma_0 = 0) = 3 \times 10^{-16}$ Pa/s and $c(\sigma_0 = 0) = 2 \times 10^{-15}$ Pa/s in proportion with the prestress σ_0 (Fig. 6 *B*); however, $\frac{a}{c} = \text{const}$. This shows that

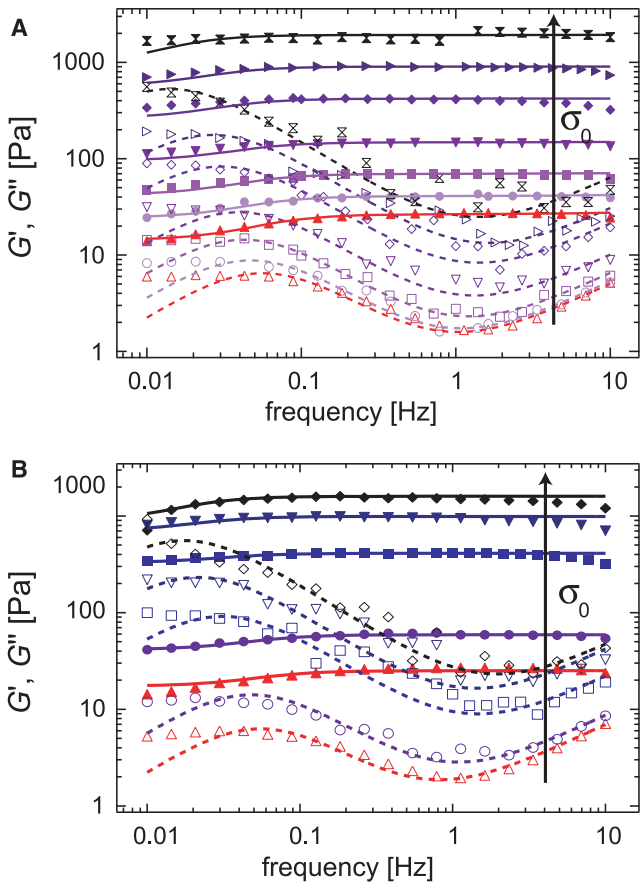

FIGURE 5 Frequency response of actin/HMM networks ($c_a = 9.5\ \mu$M) at distinct levels of prestress σ_0. Solid symbols denote $G'(f)$, open symbols denote $G''(f)$. The solid and dashed lines represent the model used to evaluate the macromechanical response, as described in Lieleg et al. (13). (*A*) $R = 0.1$: $\sigma_0 = 0$ Pa (*upright triangles*), 0.5 Pa, 1 Pa, 2 Pa, 5 Pa, 10 Pa, and $\sigma_0 = 20$ Pa (*crosses*), (*B*) $R = 0.2$: $\sigma_0 = 0$ Pa (*upright triangles*), 1 Pa, 5 Pa, 10 Pa, and $\sigma_0 = 15$ Pa (*diamonds*). The maximum level of prestress is chosen in such a way that the networks still show complete relaxation to their original (unstressed) state upon stress release.

the amount of dissipated energy upon cross-link unbinding as well as the loss in the network elasticity are both enhanced in the presence of prestress—with the same dependence on σ_0. Interestingly, the same scaling behavior is observed for the parameter $d(\sigma_0 = 0) = 0.08$ Pa, which describes the high frequency regime that is dominated by the fluctuations of single filaments.

Concomitant with the enhanced network elasticity, an exponential decrease of the apparent cross-linker off-rate is observed for both cross-linker densities studied here (Fig. 6 *C*). In an isotropically cross-linked actin network, the macroscopic stress will be transduced to single actin/ABP bonds following the geometry of the network. Depending on the orientation of the cross-link relative to the direction of the applied force, a distribution of force vectors will be present. Partially, they will stabilize or destabilize the bonds. With the simplified assumption that stabilizing and destabilizing

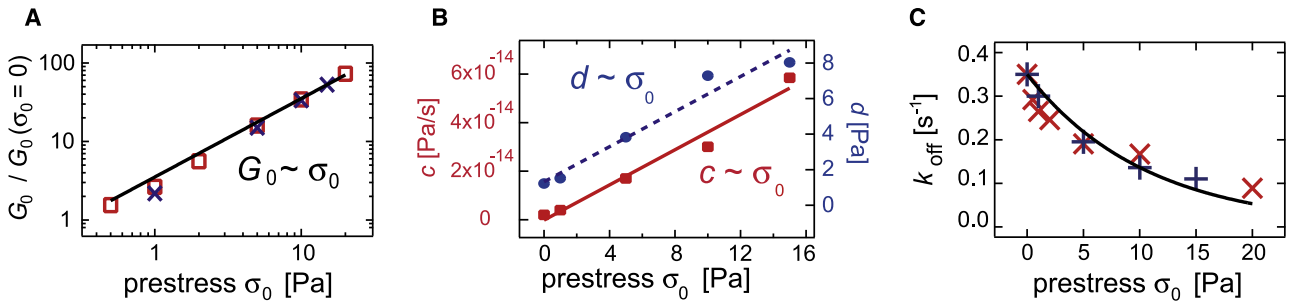

FIGURE 6 Fitting parameters for prestressed actin/HMM networks as obtained for the data sets depicted in Fig. 5, *A* and *B*. (*A*) Enhancement of the network elasticity $G_0/G_0(\sigma_0 = 0)$ as a function of prestress σ_0. A linear relation is observed for both cross-linker densities ($R = 0.1$ (*squares*) and $R = 0.2$ (*crosses*)). (*B*) Stress relaxation parameter c and single filament relaxation parameter d increase linear with the prestress σ_0. (*C*) Cross-linker off-rate k_{off} as a function of prestress for two different actin/HMM networks ($R = 0.1$ (×) and $R = 0.2$ (+)).

forces of identical magnitude are equally probable, a decrease in the apparent cross-linker off-rate of the network with increasing force can be rationalized (see Appendix). With that an Arrhenius law, $k_{off}^F = k_{off}^0 \times \exp(-\sigma_0/\sigma^*)$, can be fitted to the observed decay of k_{off} in Fig. 6 *C*. Here, k_{off}^F and k_{off}^0 denote the cross-linker off-rate in the presence and absence of external force, F, and σ^* is the characteristic decay stress. The magnitude of force that is transduced to a single bond is given by the level of prestress as $F \sim \sigma_0$. In a Bell model (27), the characteristic bond length is described by the position of the transition state Δx. As a consequence, the following relation can be assumed to hold: $\frac{\sigma_0}{\sigma^*} = F \times \Delta x / k_B T$. To extract the bond length Δx from this relation, the ratio F/σ_0 has to be determined for any level of prestress. We assume that F/σ_0 depends only on the network geometry and not on the magnitude of the applied force. Therefore, the point of bond rupturing is chosen to determine this ratio since the rupture event is experimentally accessible. For actin/HMM networks, the rupture force of a single bond was determined to be ≈8 pN, and the corresponding rupture stress is $\sigma_0 \approx$ 30–40 Pa (6) for $R = 0.14$. Hence, the bond length Δx can directly be calculated from the decay stress $\sigma^* = (10.6 \pm 1.3)$ Pa to be $\Delta x \approx (1.9 \pm 0.7)$ nm. This is in excellent agreement with literature values obtained from microscopic studies of the actin/HMM bond. There, a bond length $\Delta x_\perp = 0.5$ nm (28) and $\Delta x_\parallel = 2$ nm (29) was reported, depending on whether the force was applied orthogonally to the binding direction (28) or in a parallel manner (29). Indeed, our simple considerations give a reasonable value $\Delta x_\perp < \Delta x < \Delta x_\parallel$. This might reflect the fact that, in an isotropically cross-linked network, a distribution of various force directions is present. However, simulations might be necessary to determine this force distribution in detail.

In conclusion, we have demonstrated that the microscopic interaction potential of an actin/ABP bond determines the macroscopic viscoelastic response of a transiently cross-linked actin network. The transient character of actin/ABP bonds gives rise to a delicate sensitivity of cytoskeletal mechanics toward external or internal forces. This might provide a central mechanism that living cells can exploit for mechanosensing tasks. Because distinct ABPs differ in their biochemical properties such as the off-rate, binding energy, or bond length, the corresponding actin/ABP interaction potentials provide a formidable basis to tailor the dynamic viscoelastic response of the cytoskeleton. Vice versa, we have shown that the interaction potential of the actin/HMM bond can be characterized by analyzing solely the macroscopic viscoelastic response of a cross-linked actin network. A selection of appropriate measuring protocols in combination with a microscopic model allows us to determine the off-rate, binding energy, and bond length of the actin/HMM unbinding process. Collective phenomena do not have to be accounted for in isotropically cross-linked networks, as the parameters determined from the macroscopic network response are in excellent agreement with single molecule experiments. The off-rate of the actin/HMM bond is very similar to those of other actin/ABP bonds, such as actin/fascin (30), actin/α-actinin (31), or actin/filamin (31). This suggests that unbinding of cross-linking molecules is an ubiquitous mechanism, which dictates the dynamic properties of isotropically cross-linked actin networks at biologically relevant timescales. Indeed, the frequency responses reported in a recent study on reconstituted actin networks cross-linked by α-actinin-4 (23) fit qualitatively very well into the approach presented here. Our results, however, set the basis to quantitatively address the microscopic principles underlying the macromechanical properties of more complicated networks, be it purely bundled or composite networks as used by living cells.

APPENDIX

Fitting parameters

We conduct an iterative fitting procedure. First, each data set is fitted freely. For parameters, which return very similar values, their mean value is fixed and used for the whole data set. This strategy is applied for all data sets discussed in this article.

R-series

A best fit of the data set returns an almost linear dependence of the cross-link density N on the experimentally controlled parameter R as compiled in Table 1. $N \sim R^{1.1}$ is obtained in excellent agreement with the former experimental

TABLE 1 Fitting parameters used in Fig. 3 *A* as a function of the experimental control parameter *R* for a fixed actin concentration $c_a = 19\ \mu M$

		$R = 0.0076$	$R = 0.0152$	$R = 0.0385$	$R = 0.0714$	$R = 0.143$
N	[10^{14}]	0.39	0.66	1.69	4.19	8.31
k_{off}	[s^{-1}]	0.3	0.3	0.3	0.3	0.3
a	[10^{-16} Pa/s]	3	3	3	3	3
b	[Pa]	0.4	0.4	0.4	0.4	0.4
c	[10^{-15} Pa/s]	2	2	2	2	2
d	[Pa]	0.7	0.7	0.7	0.7	0.7
f_0	[Hz]	1	1	1	1	1

finding $G_0 \sim R^{1.2}$ (6,20). Note that the absolute values of N and a (and thus also c) are ambiguous; only the product $a \times N$ (or $c \times N$) is directly set by the fit result. However, a is globally fixed for all un-prestressed data sets shown and the scaling relations discussed in the article as well as all conclusions drawn remain unaffected by the ambiguity in the absolute values of these parameters.

c_a-series

Very similar parameters as used for the R-series are also applied for the reproduction of the data set shown in Fig. 3 *B*. The corresponding values are compiled in Table 2.

T-series

For the temperature series depicted in Fig. 4 *A*, $k_{off} = 0.3\ s^{-1}$ is used together with $a = 3 \times 10^{-16}$ Pa/s, $b = 0.4$ Pa, $c = 2 \times 0^{-15}$ Pa/s, and $d = 0.3$ Pa. N is varied linearly with G_0, which is depicted in Fig. 4 *B*.

Prestress-series

Both prestress series depicted in Fig. 5, *A* and *B*, use constant N values and $f_0 = 1$ Hz. The dependence of all other parameters is explicitly discussed in the article.

Apparent off-rate in a cross-linked network under prestress

In prestressed actin/HMM networks a decrease in the apparent off-rate with respect to external prestress is observed (Fig. 6 *C*). In single molecule experiments with rigor HMM, such a decrease of the cross-link off-rate in the presence of mechanical load has already been reported (29)—consistent with a catch-slip mechanism of the actin/HMM bond. However, a simple approximation shows that in a network of cross-linked actin filaments the network geometry gives rise to a decrease in the apparent cross-linker off-rate in the presence of mechanical load. Moreover, this decrease in the apparent cross-linker off-rate is independent of the particular binding mechanism and therefore a geometrical effect.

In the following, the effective off-rate is calculated for a model system where the cross-links experience forces of constant magnitude but with random algebraic sign: $F^{\pm} = \pm F_0 \sim \pm\sigma_0$. This extremely simplified model is able to rationalize the counterintuitive dependence of the off-rate on external force—at least in a qualitative manner. The actual force distribution will be much more complex.

If the forces $F^{\pm} = \pm F_0 \sim \pm\sigma_0$ load an ensemble of N_Σ bonds, two different off-rates $k_{off}^{+} = k_{off} \times \exp(+ F \times \Delta x/k_BT)$ and $k_{off}^{-} = k_{off} \times \exp(-F \cdot \Delta x/k_BT)$ emerge: $N_\Sigma = N^+ + N^-$. Here N^+ denotes the number of cross-links with enhanced off-rate (destabilized fraction) and N^- denotes the number of cross-links with lowered off-rate (stabilized fraction).

This defines an effective off-rate k_{off}^{eff} for the whole ensemble of N_Σ cross-links:

$$k_{off}^{eff} \times N_\Sigma = k_{off}^{+} \times N^+ + k_{off}^{-} \times N^-. \quad (3)$$

For constant on-rates (note that this assumption is reasonable since, during the binding process, a cross-linking protein does not feel any external force acting on the actin filaments), $k_{on}^{+} = k_{on}^{-}$, the two populations N^+ and N^- equilibrate according to the difference in their off-rates:

$$\frac{N^+}{N^-} = \frac{k_{off}^{-}}{k_{off}^{+}}. \quad (4)$$

Eliminating N^- in Eq. 4 results in

$$N^+ = N_\Sigma \times \frac{k_{off}^{-}}{k_{off}^{+} + k_{off}^{-}}. \quad (5)$$

Together with Eqs. 3 and 4, one obtains

$$k_{off}^{eff} = 2 \times \frac{k_{off}^{+} \times k_{off}^{-}}{k_{off}^{+} + k_{off}^{-}}, \quad (6)$$

which results in the apparent off-rate

$$k_{off}^{eff} = 2 \times \frac{k_{off}^{0}}{\exp(+ F \times \Delta x/k_BT) + \exp(-F \times \Delta x/k_BT)}, \quad (7)$$

which can be rewritten to $k_{off}^{eff} = k_{off}^{0}/\cosh(F \times \Delta x/k_BT) < k_{off}^{0}$.

TABLE 2 Fitting parameters used in Fig. 3 *B* as a function of the experimental control parameter c_a for fixed $R = 0.1$

		$c_a = 4.75\ \mu M$	$c_a = 9.5\ \mu M$	$c_a = 19\ \mu M$	$c_a = 27.5\ \mu M$
N	[10^{14}]	0.14	1.40	7.57	2.25
k_{off}	[s^{-1}]	0.23	0.23	0.23	0.23
a	[10^{-16} Pa/s]	3	3	3	3
b	[Pa]	0.15	0.4	0.95	2.2
c	[10^{-15} Pa/s]	2	2	2	2
d	[Pa]	0.3	0.8	1.9	4.4
f_0	[Hz]	1	1	1	1

We thank M. Rusp for the actin preparation.

Financial support of the German Excellence Initiatives via the "Nanoinitiative Munich" (NIM), the "Munich-Centre for Advanced Photonics (MAP)", and by the DFG through Grant No. Ba2029/8-1 is gratefully acknowledged. O. Lieleg acknowledges support from CompInt in the framework of the ENB Bayern.

REFERENCES

1. Xu, J., D. Wirtz, and T. Pollard. 1998. Dynamic cross-linking by α-actinin determines the mechanical properties of actin filament networks. *J. Biol. Chem.* 273:9570–9576.

2. Wang, N., I. Tolic-Norrelykke, J. Chen, S. Mijailovich, J. Butler, et al. 2002. Cell prestress. I. Stiffness and prestress are closely associated in adherent contractile cells. *Am. J. Physiol. Cell Physiol.* 282:C606–C616.

3. Bausch, A. R., and K. Kroy. 2006. A bottom-up approach to cell mechanics. *Nature Phys.* 2:231–238.

4. Head, D. A., A. Levine, and F. MacKintosh. 2003. Distinct regimes of elastic response and deformation modes of cross-linked cytoskeletal and semiflexible polymer networks. *Phys. Rev. E Stat. Nonlin. Soft Matter Phys.* 68:061907–1–15.

5. Wilhelm, J., and E. Frey. 2003. Elasticity of stiff polymer networks. *Phys. Rev. Lett.* 91:108103.

6. Tharmann, R., M. M. A. E. Claessens, and A. R. Bausch. 2007. Viscoelasticity of isotropically cross-linked actin networks. *Phys. Rev. Lett.* 98:088103.

7. Heussinger, C., and E. Frey. 2006. Floppy modes and non-affine deformations in random fiber networks. *Phys. Rev. Lett.* 97:105501.

8. Lieleg, O., M. M. A. E. Claessens, C. Heussinger, E. Frey, and A. R. Bausch. 2007. Mechanics of bundled semiflexible polymer networks. *Phys. Rev. Lett.* 99:088102.

9. Lieleg, O., and A. R. Bausch. 2007. Cross-linker unbinding and self-similarity in bundled cytoskeletal networks. *Phys. Rev. Lett.* 99: 158105.

10. Gardel, M. L., J. H. Shin, F. C. MacKintosh, L. Mahadevan, P. Matsudaira, et al. 2004. Elastic behavior of cross-linked and bundled actin networks. *Science.* 304:1301–1305.

11. Gardel, M. L., F. Nakamura, J. H. Hartwig, J. C. Crocker, T. P. Stossel, et al. 2006. Prestressed F-actin networks cross-linked by hinged filamins replicate mechanical properties of cells. *Proc. Natl. Acad. Sci. USA.* 103:1762–1767.

12. Semmrich, C., J. Glaser, R. Merkel, A. R. Bausch, and K. Kroy. 2007. Glass transition and rheological redundancy in F-actin solutions. *Proc. Natl. Acad. Sci. USA.* 104:20199–20203.

13. Lieleg, O., M. M. A. E. Claessens, Y. Luan, and A. Bausch. 2008. Transient binding and dissipation in cross-linked actin networks. *Phys. Rev. Lett.* 101:108101.

14. Wagner, B., R. Tharmann, I. Haase, M. Fischer, and A. R. Bausch. 2006. Cytoskeletal polymer networks: the molecular structure of cross-linkers determines macroscopic properties. *Proc. Natl. Acad. Sci. USA.* 103:13974–13978.

15. Evans, E. 1998. Energy landscapes of biomolecular adhesion and receptor anchoring at interfaces explored with dynamic force spectroscopy. *Faraday Discuss.* 111:1–16.

16. Schlierf, M., and M. Rief. 2006. Single-molecule unfolding force distributions reveal a funnel-shaped energy landscape. *Biophys. J.* 90: L33–L35.

17. Spudich, J. A., and S. Watt. 1971. Regulation of rabbit skeletal muscle contraction. 1. Biochemical studies of interaction of tropomyosin-troponin complex with actin and proteolytic fragments of myosin. *J. Biol. Chem.* 246:4866–4871.

18. Kurokawa, H., W. Fujii, K. Ohmi, T. Sakurai, and Y. Nonomura. 1990. Simple and rapid purification of brevin. *Biochem. Biophys. Res. Commun.* 168:451–457.

19. Uhde, J., M. Keller, and E. Sackmann. 2004. Internal motility in stiffening actin-myosin networks. *Phys. Rev. Lett.* 93:268101.

20. Luan, Y., O. Lieleg, B. Wagner, and A. R. Bausch. 2008. Micro- and macrorheological properties of isotropically cross-linked actin networks. *Biophys. J.* 94:688–693.

21. Marston, S. B. 1982. The rates of formation and dissociation of actin-myosin complexes. *Biochem. J.* 203:453–460.

22. MacKintosh, F. C., J. Käs, and P. A. Janmey. 1995. Elasticity of semiflexible biopolymer networks. *Phys. Rev. Lett.* 75:4425–4428.

23. Volkmer-Ward, S. M., A. Weins, M. R. Pollak, and D. A. Weitz. 2008. Dynamic viscoelasticity of actin cross-linked with wild-type and disease-causing mutant α-actinin-4. *Biophys. J.* 95:4915–4923.

24. Highsmith, S. 1977. The effects of temperature and salts on myosin subfragment-1 and F-actin association. *Arch. Biochem. Biophys.* 180: 404–408.

25. Tempel, M., G. Isenberg, and E. Sackmann. 1996. Temperature-induced sol-gel transition and microgel formation in α-actinin cross-linked actin networks: a rheological study. *Phys. Rev. E Stat. Phys. Plasmas Fluids Relat. Interdiscip. Topics.* 54:1802–1810.

26. Evans, E., and K. Ritchie. 1997. Dynamic strength of molecular adhesion bonds. *Biophys. J.* 72:1541–1555.

27. Bell, G. I. 1978. Models for specific adhesion of cells to cells. *Science.* 200:618–627.

28. Nishizaka, T., R. Seo, H. Tadakuma, K. Kinosita, and S. Ishiwata. 2000. Characterization of single actomyosin rigor bonds: load dependence of lifetime and mechanical properties. *Biophys. J.* 79:962–974.

29. Guo, B., and W. H. Guilford. 2006. Mechanics of actomyosin bonds in different nucleotide states are tuned to muscle contraction. *Proc. Natl. Acad. Sci. USA.* 103:9844–9849.

30. Aratyn, Y., T. Schaus, E. Taylor, and G. Borisy. 2007. Intrinsic dynamic behavior of fascin in filopodia. *Mol. Biol. Cell.* 18:3928–3940.

31. Goldmann, W., and G. Isenberg. 1993. Analysis of filamin and α-actinin binding to actin by the stopped flow method. *FEBS Lett.* 336:408–410.

32. Reference deleted in proof.